Action-Potential Modulation During Axonal Conduction

Takuya Sasaki, *et al.*

Science **331**, 599 (2011);
DOI: 10.1126/science.1197598

Action-Potential Modulation During Axonal Conduction

Takuya Sasaki,[1] Norio Matsuki,[1] Yuji Ikegaya[1,2]*

Once initiated near the soma, an action potential (AP) is thought to propagate autoregeneratively and distribute uniformly over axonal arbors. We challenge this classic view by showing that APs are subject to waveform modulation while they travel down axons. Using fluorescent patch-clamp pipettes, we recorded APs from axon branches of hippocampal CA3 pyramidal neurons ex vivo. The waveforms of axonal APs increased in width in response to the local application of glutamate and an adenosine A_1 receptor antagonist to the axon shafts, but not to other unrelated axon branches. Uncaging of calcium in periaxonal astrocytes caused AP broadening through ionotropic glutamate receptor activation. The broadened APs triggered larger calcium elevations in presynaptic boutons and facilitated synaptic transmission to postsynaptic neurons. This local AP modification may enable axonal computation through the geometry of axon wiring.

Contrary to the prevailing notion of the digital-like uniformity of action potentials (APs), recent evidence has shown that APs (or axons) are capable of conveying information in a graded analog manner (*1*–*4*). It remains unknown, however, whether already-generated APs can be modulated during axonal conduction. Because axons express various types of transmitter receptors and ion channels, in particular on their presynaptic terminals (*5*, *6*), local alterations in the ion conductance of aligned synapses along an axon may modify the waveforms of APs traveling down its length.

We recorded CA3 pyramidal cells (PCs) in hippocampal slice cultures, unless otherwise specified (*7*). Alexa Fluor–loaded patch pipettes were used to visualize their axons (Fig. 1A). An axonal branch that was 150 to 700 μm away from the axon hillock was targeted for cell-attached recording with a fluorophore-coated pipette under spinning-disk confocal visualization (*8*). APs were evoked by current injection into the soma and were extracellularly captured at the axon as sharp sink potentials. Extracellularly recorded APs (eAPs) were likely to be a mixture of the inverse of intracellularly recorded APs (iAPs) and their derivatives (fig. S1).

Glutamate or γ-aminobutyric acid (GABA) was locally puff-applied to the axon midway between two patch-clamp pipettes. The effective radius of this local application was less than 100 μm, as confirmed by diffusion of coapplied Alexa Fluor dye. Application of 10 μM glutamate induced a rapid and reversible increase in the half-maximal duration of eAPs that were recorded within 200 μm of the site of glutamate administration (Fig. 1B, $t_{10} = 5.44$, $P = 0.0003$ paired t test). This low concentration of glutamate did not change the iAP width recorded at the soma (Fig. 1B, –0.61 ± 1.6%, $t_{10} = 0.28$, $P = 0.78$) or the somatic resting membrane potential (–0.4 ± 0.8 mV of change, $t_{10} = 0.53$, $P = 0.60$). It also did not affect the spike activity of nearby neurons (fig. S2). Unlike glutamate, 1 mM GABA had no significant effect on the eAP width (Fig. 1C, $t_5 = 1.03$, $P = 0.34$).

Glutamate did not broaden eAPs in the presence of 10 μM 6-cyano-7-nitroquinoxaline-2,3-dione (CNQX), a non–*N*-methyl-D-aspartate (NMDA) receptor antagonist (Fig. 1C, $t_6 = 1.31$, $P = 0.23$), but it did in the presence of 50 μM L,D-2-amino-5-phosphonopentanoic acid (AP5), an NMDA receptor antagonist (MCPG) (Fig. 1C, $t_5 = 3.47$, $P = 0.02$), and 500 μM (*S*)-α-methyl-4-carboxyphenylglycine, a group I/II metabotropic glutamate receptor antagonist (Fig. 1C, $t_5 = 7.42$, $P = 0.0006$). The eAP broadening was not affected by bath application of a glutamate transporter inhibitor [100 μM DL-threo-β-benzyloxyaspartic acid (TBOA)] (Fig. 1C, $t_3 = 4.00$, $P = 0.028$), preincubation with a vesicle fusion inhibitor [10 nM tetanus toxin (TeNT)] (Fig. 1C, $t_4 = 4.06$, $P = 0.0097$), or intracellular injection of a Ca^{2+} chelator [20 mM 1,2-bis(*o*-aminophenoxy)ethane-*N*,*N*,*N*',*N*'-tetraacetic acid (BAPTA)] into the somata (Fig. 1C, $t_3 = 4.19$, $P = 0.024$). Thus, glutamate appears to

[1]Laboratory of Chemical Pharmacology, Graduate School of Pharmaceutical Sciences, University of Tokyo, Tokyo 113-0033, Japan. [2]Precursory Research for Embryonic Science and Technology, Japan Science and Technology Agency, 4-1-8 Honcho Kawaguchi, Saitama 332-0012, Japan.

*To whom correspondence should be addressed. E-mail: ikegaya@mol.f.u-tokyo.ac.jp

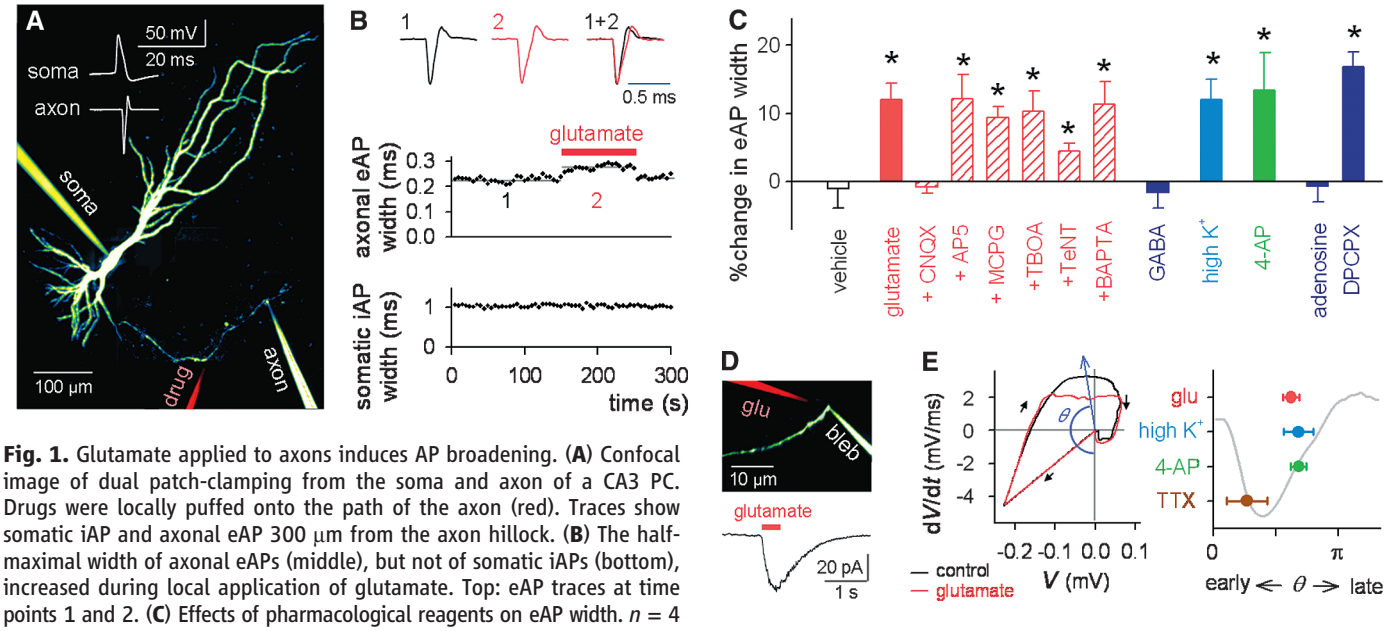

Fig. 1. Glutamate applied to axons induces AP broadening. (**A**) Confocal image of dual patch-clamping from the soma and axon of a CA3 PC. Drugs were locally puffed onto the path of the axon (red). Traces show somatic iAP and axonal eAP 300 μm from the axon hillock. (**B**) The half-maximal width of axonal eAPs (middle), but not of somatic iAPs (bottom), increased during local application of glutamate. Top: eAP traces at time points 1 and 2. (**C**) Effects of pharmacological reagents on eAP width. $n = 4$ to 7 slices, $^*P < 0.05$, paired t test. (**D**) Glutamate-induced inward current in whole-cell recorded axon blebs. (**E**) Phase-space analysis of an eAP waveform. (Left) An eAP was plotted in the space of V versus dV/dt, where V represents the eAP voltage at a given time. The phase θ (blue arrow) was determined to maximize the difference between the orbits of eAPs before (black) and during drug application (red). Right: The θ values were similar for eAPs modulated by glutamate, high-K^+ depolarization, or 4-AP, but not by TTX. $n = 4$ or 5 slices.

modulate APs by depolarizing axons through AMPA receptor activation rather than by triggering transmitter release or Ca^{2+}-dependent cellular signals. Consistent with this, 20 mM K^+ applied to axons induced eAP broadening (Fig. 1C, t_3 = 4.59, P = 0.0037).

In CA3 PCs of acute hippocampal slices, the cut ends (blebs) of the axons were whole-cell patch-clamped (*2*). Puffing glutamate to the blebs elicited an inward current of 38.2 ± 5.6 pA at a holding potential of –70 mV (Fig. 1D, n = 3 blebs).

To investigate the mechanisms underlying the AP broadening, we analyzed the eAP waveform in the phase space of V versus dV/dt (Fig. 1E). The orbits of control and glutamate-broadened eAPs separated maximally in a late phase during their temporal evolution. The late-phase modulation was replicated by high-K^+ depolarization and pharmacological blockade of the Kv1 family of voltage-activated K^+ channels by 10 μM 4-aminopyridine (4-AP), whereas the earlier phase was sensitive to partial blockade of voltage-activated Na^+ channels by 10 nM tetrodotoxin (TTX). Thus, depolarization-induced K^+ channel inactivation (*1*, *4*) is likely to underlie the AP broadening.

To determine the extent of glutamate's influence, we patched axons at various distances downstream of the site of glutamate administration. eAP broadening was more evident at axons nearer the site of glutamate administration, and the decay constant was found to be 223 μm (Fig. 2A, n = 17 axons). Likewise, the eAP-broadening effect was not observed at distances greater than 250 μm upstream from the glutamate spot (t_4 = 0.51, P = 0.60) or at axon branches other than those that received glutamate puffs (Fig. 2B, t_5 = 0.66, P = 0.54).

Adenosine A_1 receptors are expressed in presynaptic axons (*9*). Local application of 1 mM adenosine did not modulate eAPs (Fig. 1C, t_5 = 0.33, P = 0.75), but 100 μM 8-cyclopentyl-1,3-dipropylxanthine (DPCPX), an A_1 receptor antagonist, increased the eAP width (Fig. 1C, t_5 = 7.61, P = 0.0006), suggesting tonic AP suppression by endogenous adenosine.

We next sought to determine whether AP modulation affects presynaptic Ca^{2+} dynamics (fig. S3). Oregon Green BAPTA-1 (OGB1), a Ca^{2+} indicator, was intracellularly injected into PCs. In some cases, its AM form was bolus-injected into the stratum oriens. Intra-axonally diffused dye was confocally imaged from individual presynaptic boutons. APs induced a transient rise in Ca^{2+} fluorescence in the boutons. The increases in Ca^{2+} were further enhanced by glutamate applied to axons. This enhancement did not occur in the presence of CNQX and AP5. DPCPX, but not adenosine, also enhanced the Ca^{2+} response.

To investigate whether AP broadening modulates synaptic efficacy, we recorded synaptically connected pairs of CA3 PCs. In each experiment, we identified the axon branch that was responsible for the synaptic connection by sequentially puffing 1 μM TTX onto individual Alexa-visualized axon collaterals (Fig. 3A). Focal activation of the identified branch by glutamate application increased the mean amplitude of unitary excitatory postsynaptic currents (uEPSCs) in the downstream postsynaptic neurons (Fig. 3, B and C, t_{11} = 3.49, P = 0.006) and decreased the failure of synaptic transmission (fig. S4) and the paired-pulse response ratio (PPR), defined as the second uEPSC amplitude divided by the first evoked by two 50-ms-interval stimuli (Fig. 3D, t_4 = 4.31, P = 0.01). DPCPX (Fig. 3D, t_5 = 5.70, P = 0.002), but not adenosine (Fig. 3D, t_5 =1.38, P = 0.23), increased the uEPSC amplitude. 4-AP also increased synaptic efficacy (Fig. 3D, t_5 = 5.46, P = 0.003) and decreased PPR (t_5 = 7.81, P = 0.0006).

Most local axons of CA3 PCs are unmyelinated, and their shafts and presynaptic varicosities contact astrocytes (*10*). These periaxonal astrocytes may modulate APs through the release of gliotransmitters. Astrocytes residing near the axons of CA3 PCs (150 to 400 μm from axon

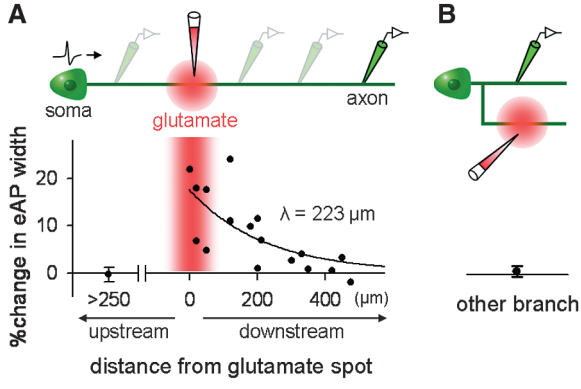

Fig. 2. The AP-broadening effect reaches beyond the glutamate-activated region. **(A)** A glutamate-induced increase in axonal eAP width is plotted against the path distance between the glutamate puff and the cell-attached recording positions. Red indicates the puffed area (<100 μm ϕ). The line was best fit to a single exponential decay (R^2 = 0.50, P = 0.01, n = 17 axon recordings). The decay constant λ (223 μm) was smaller than the axon length constant reported previously (~500 μm) (*2*–*4*). Extracellular recording of APs may underestimate the effect of AP broadening. **(B)** Glutamate applied to axon branches in different locations than the recording site had no effect. n = 6 axons.

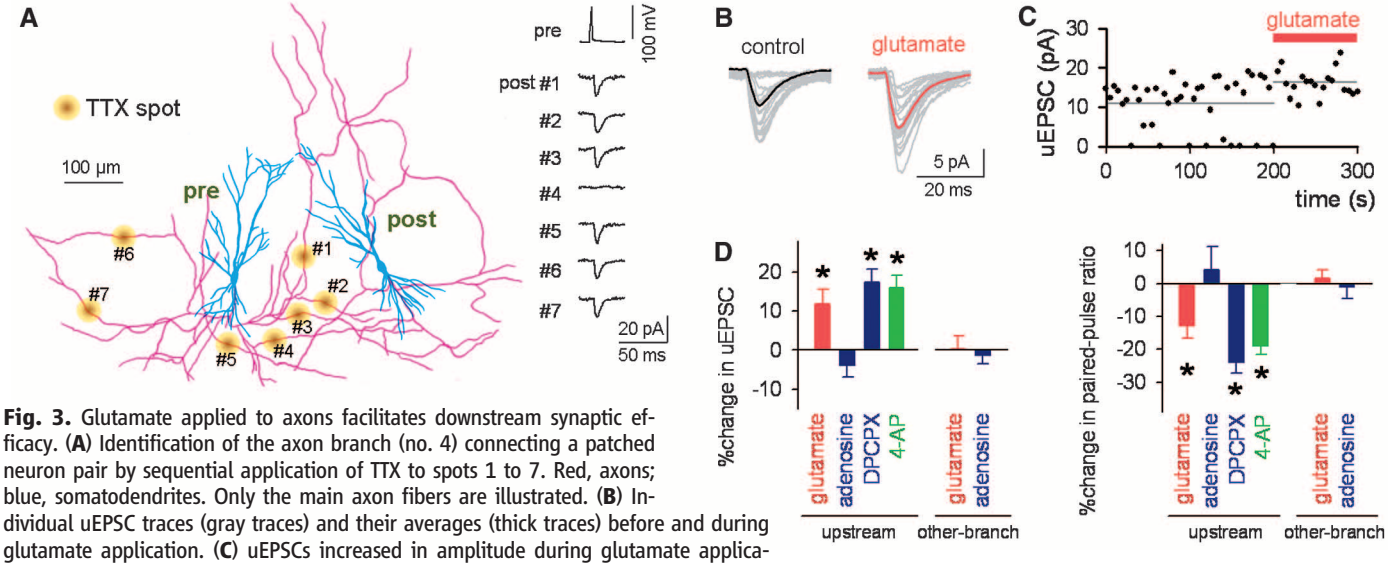

Fig. 3. Glutamate applied to axons facilitates downstream synaptic efficacy. **(A)** Identification of the axon branch (no. 4) connecting a patched neuron pair by sequential application of TTX to spots 1 to 7. Red, axons; blue, somatodendrites. Only the main axon fibers are illustrated. **(B)** Individual uEPSC traces (gray traces) and their averages (thick traces) before and during glutamate application. **(C)** uEPSCs increased in amplitude during glutamate application. **(D)** Effects of local drug application on synaptic responses evoked by single-pulse (left) and paired-pulse (right) stimulation. n = 5 to 12 slices, *P < 0.05, paired t test.

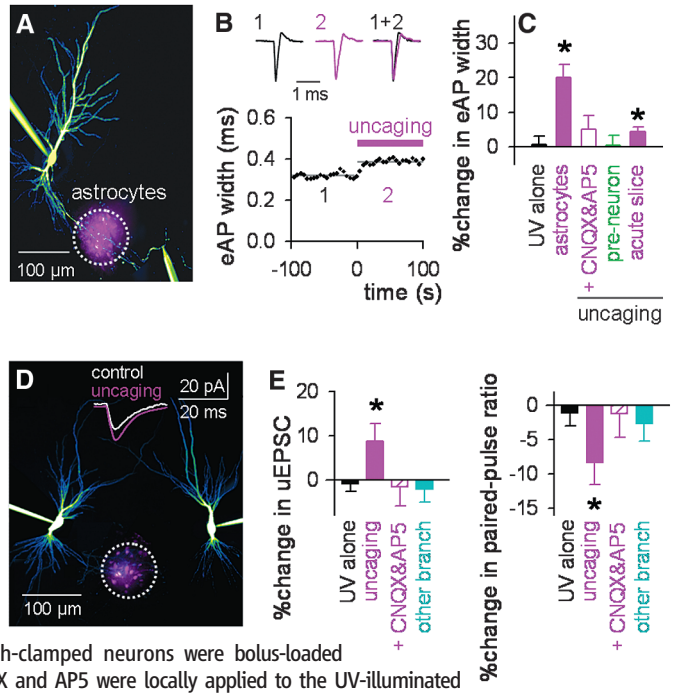

Fig. 4. Ca^{2+} uncaging in periaxonal astrocytes broadens APs and facilitates downstream synaptic transmission. (**A**) Astrocytes (magenta) bolus-loaded with NP-EGTA-AM near the axon whose soma and downstream axon (green) were patch-clamp–recorded. UV illuminated the circled area. (**B**) Photolysis of NP-EGTA induced axonal eAP broadening. Inset at top: eAPs at time points 1 and 2. (**C**) Summarized data, including slices that were not loaded with NP-EGTA-AM (UV alone) and slices in which the presynaptic neuron was intracellularly loaded with NP-EGTA (pre-neuron). (**D**) Astrocytes near the axon connecting two patch-clamped neurons were bolus-loaded with NP-EGTA-AM. (**E**) CNQX and AP5 were locally applied to the UV-illuminated area. UV was also applied to unloaded slices (UV alone) and slices in which NP-EGTA-AM was bolus-loaded into the astrocytes around irrelevant axon branches (other branch). $n = 6$ to 19 slices, $^*P < 0.05$, paired t test.

hillocks) were bolus-loaded with OGB1-AM and *O*-nitrophenyl-ethylene glycol tetraacetic acid AM (NP-EGTA-AM), a membrane-permeating caged-Ca^{2+} compound (Fig. 4A). Astrocytes were morphologically and immunohistochemically identified (fig. S5) and preferentially loaded with NP-EGTA-AM (*11*). Photolysis of caged Ca^{2+} by an ultraviolet (UV) pulse (120 μm in diameter) elicited oscillatory Ca^{2+} fluctuations in the illuminated astrocytes, which persisted for several minutes (fig. S6D). The activity did not propagate to neighboring, nonilluminated astrocytes. UV illumination did not activate astrocytes that were not loaded with NP-EGTA (fig. S6E, UV alone).

Ca^{2+} uncaging in astrocytes increased the duration of eAPs recorded at downstream axons within 200 μm of the UV spot (Fig. 4, B and C, $t_6 = 5.90$, $P = 0.001$). The same effect was observed in axons of CA3 PCs of acute hippocampal slices (a 4.5 ± 1.0% increase in eAP width, $t_3 = 4.83$, $P = 0.02$). UV pulses did not induce eAP broadening in the presence of CNQX and AP5 (Fig. 4C, $t_4 = 1.40$, $P = 0.23$) or in slices without NP-EGTA-AM loading (Fig. 4C, $t_4 = 0.38$, $P = 0.73$). We rule out the possibility that UV-induced Ca^{2+} elevation in NP-EGTA–loaded axons caused the eAP broadening, because UV illumination of axons of presynaptic neurons injected with 200 μM NP-EGTA failed to broaden eAPs (Fig. 4C, $t_4 = 0.02$, $P = 0.98$). Astrocyte activation increased the amplitude of AP-triggered Ca^{2+} transients in presynaptic boutons, an effect that was not observed in the presence of CNQX and AP5 or in slices without NP-EGTA loading (fig. S7).

To examine whether the Ca^{2+} activity of periaxonal astrocytes facilitated downstream synaptic efficacy, astrocytes near the presynaptic axon branches connecting patched PC pairs were loaded with NP-EGTA-AM (Fig. 4D). UV activation of these astrocytes amplified uEPSCs in the postsynaptic neurons (Fig. 4E, $t_{18} = 2.27$, $P = 0.03$) and reduced PPR ($t_{15} = 2.54$, $P = 0.02$). Both effects were blocked by coapplication of CNQX and AP5 to the UV-illuminated area (Fig. 4E, $t_8 = 0.24$, $P = 0.81$). Neither UV illumination alone (Fig. 4E, $t_9 = 0.97$, $P = 0.36$) nor UV activation of astrocytes on irrelevant axon branches ($t_5 = 0.82$, $P = 0.45$) facilitated synaptic transmission. To examine the impact of single astrocyte activation, we injected NP-EGTA into a periaxonal astrocyte through a whole-cell pipette (fig. S8A). In 5 of 13 experiments, photostimulation led to a modest but significant increase in uEPSC efficacy as well as a decrease in PPRs. When the data for the entire sample were analyzed statistically, these effects were still significant (fig. S8B). Ca^{2+} uncaging in the axons of NP-EGTA–loaded presynaptic neurons failed to modulate synaptic transmission.

We demonstrated that activation of AMPA receptors directly or indirectly causes a depolarizing current in axons and thereby broadens APs during axonal conduction. The endogenous agonist glutamate appears to be provided by periaxonal astrocytes [but see (*12*)]. Astrocytes are known to regulate local synaptic transmission (*13*–*16*), but this work reveals that they are far more influential than expected, because the length constant of the axon cable (*2*–*4*) exceeds their cell diameter. Our findings derived from experimentally designed ex vivo systems using artificial stimulation should be extrapolated to other systems with caution. Elucidating their physiological relevance requires further investigation.

References and Notes

1. Y. Shu, Y. Yu, J. Yang, D. A. McCormick, *Proc. Natl. Acad. Sci. U.S.A.* **104**, 11453 (2007).
2. Y. Shu, A. Hasenstaub, A. Duque, Y. Yu, D. A. McCormick, *Nature* **441**, 761 (2006).
3. H. Alle, J. R. Geiger, *Science* **311**, 1290 (2006).
4. M. H. Kole, J. J. Letzkus, G. J. Stuart, *Neuron* **55**, 633 (2007).
5. K. W. Schicker, M. M. Dorostkar, S. Boehm, *Curr. Mol. Pharmacol.* **1**, 106 (2008).
6. H. S. Engelman, A. B. MacDermott, *Nat. Rev. Neurosci.* **5**, 135 (2004).
7. Materials and methods are available as supporting material on *Science* Online.
8. D. Ishikawa *et al.*, *Neural Netw.* **23**, 669 (2010).
9. R. A. Cunha, *Neurochem. Int.* **38**, 107 (2001).
10. R. Ventura, K. M. Harris, *J. Neurosci.* **19**, 6897 (1999).
11. Q. S. Liu, Q. Xu, G. Arcuino, J. Kang, M. Nedergaard, *Proc. Natl. Acad. Sci. U.S.A.* **101**, 3172 (2004).
12. N. B. Hamilton, D. Attwell, *Nat. Rev. Neurosci.* **11**, 227 (2010).
13. J. Kang, L. Jiang, S. A. Goldman, M. Nedergaard, *Nat. Neurosci.* **1**, 683 (1998).
14. P. Jourdain *et al.*, *Nat. Neurosci.* **10**, 331 (2007).
15. G. Perea, A. Araque, *Science* **317**, 1083 (2007).
16. C. Henneberger, T. Papouin, S. H. Oliet, D. A. Rusakov, *Nature* **463**, 232 (2010).

17. This work was supported in part by a Grant-in-Aid for Science Research (nos. 22115003, 22650080, and 22680025) from the Ministry of Education, Culture, Sports, Science, and Technology of Japan. T.S. collected experimental data and carried out the data analysis. Y.I. conceived the project and carried out the data analysis. T.S. and Y.I. wrote the manuscript. N.M. supervised the project and provided feedback on the manuscript.

Supporting Online Material

www.sciencemag.org/cgi/content/full/331/6017/599/DC1
Materials and Methods
Figs. S1 to S8
References

9 September 2010; accepted 29 December 2010
10.1126/science.1197598